CERN - DATA HANDLING DIVISION
DD/77/2
D. Townsend
C. Piney
A. Jeavons
January 1977

OBJECT RECONSTRUCTION FROM AXIAL TOMOGRAMS

(To be submitted to Physics in Medicine and Biology)

DD/nf

OBJECT RECONSTRUCTION FROM AXIAL TOMOGRAMS

D. Townsend, C. Piney and A. Jeavons
DD Division, CERN

ABSTRACT

A major problem with the reconstruction of three-dimensional object distributions from tomographic images using Fourier transforms is the amplification of statistical noise in certain frequency components.

This paper describes the use of a generalized matrix inversion technique to limit noise amplification to a level related to the spatial resolution of the imaging system.

The reconstruction method is applied to a simulated positron camera, and results are presented on the imaging of an extended, three-dimensional object distribution. A significant improvement in the elimination of the background is achieved.

1. INTRODUCTION

Tomographic imaging techniques in medicine have been developed to obtain information about the internal structure of an object from external observations[1]. One possible method is to introduce into the object a source of radioactivity, and then to image the distribution of the radioactive emissions. A tomogram is simply this distribution for a given plane through the object with the activity distribution for all other object planes superimposed upon it, i.e., only the chosen plane is truly in focus. Early tomography[2] attempted to blur or smear all contributions except those from the chosen plane, whereas more recently, mathematical reconstruction techniques have been developed to remove these out-of-focus contributions[3]. Reconstruction can successfully eliminate the blurred background, provided three-dimensional, or depth, information is available. This is obtained by measuring not only the position in the detector of each radioactive emission, but also its direction. For single photon emission, a coded aperture or pinhole mask is placed between the object and the detector[4], whereas with positron activity the direction is measured by detecting in coincidence the two 180^{o} opposed γ-rays that emerge from each electron-positron annihilation[5].

The imaging process is expressed mathematically as a convolution of the true object distribution with the response function of the imaging system. The deconvolution, or removal of out-of-focus contributions is usually performed in Fourier space where the convolution process is equivalent to a simple product[6]. A problem can arise with this approach, because of amplification of the statistical fluctuations in the tomograms for certain frequency components. The reconstructed object distribution then becomes dominated by statistical noise, and bears little relation to the actual object distribution[7]. The basic cause of this amplification lies in the inversion of the system response function, or, in Fourier space, the system transfer function. At certain frequencies, and particularly those close to zero, the transfer function may become very small, and its inverse very large. The object distribution is derived from the product of this inverse with the corresponding frequency amplitude for the measured tomograms, so that statistical fluctuations in this frequency amplitude are scaled by the numerical value of the inverse.

The system transfer function for a set of planes is represented by a symmetric matrix for each frequency component, with elements proportional to the response at one plane to a point source in another plane. The deconvolution process requires the inverse of these matrices, and this paper describes a generalized inversion procedure, expressing each matrix as a singular value

decomposition. The form of the decomposition is suitable for placing a limit on the numerical values of the elements of the inverse, and hence on the extent of the noise amplification in the final reconstruction. In addition, by considering the transfer of statistical noise on the tomograms through the imaging system, this limit can be related to certain parameters such as spatial resolution of the data.

The generalized matrix inversion by singular value decomposition is discussed in the next Section, and the tomographic reconstruction method in Section 3. Noise amplification is studied in detail in Section 4, and Section 5 outlines the transfer of statistical noise through the imaging system and its relationship to the amplification process. The final Section describes the application of the reconstruction method to a simulated positron camera used for imaging an extended source.

2. A GENERALIZED MATRIX INVERSE

There are many ways of defining the generalized inverse of a rectangular matrix[8], but for this application only the singular value decomposition will be considered. A further limitation to square matrices is possible because the system response function may be represented by a square, symmetric matrix. The results below can always be generalized to any matrix.

Let $\underset{\sim}{v}_i$, $i = 1 \ldots n$ be the orthonormal column eigenvectors of an $n \times n$ matrix $\underset{\approx}{A}$, and let λ_i be the corresponding eigenvalues, such that

$$\underset{\approx}{A}\underset{\sim}{v}_i = \lambda_i \underset{\sim}{v}_i \tag{1}$$

Orthonormality of the $\underset{\sim}{v}_i$ implies:

$$\underset{\sim}{v}_j^T \underset{\sim}{v}_i = \delta_{ij} \quad , \quad i,j = 1 \ldots n \tag{2}$$

If $\underset{\approx}{A}$ is non-singular, then all the λ_i are non-zero and the $\underset{\sim}{v}_i$ form a basis for the space. Thus, any n-vector $\underset{\sim}{x}$ can be expressed as

$$\underset{\sim}{x} = \sum_{K=1}^{n} p_K \underset{\sim}{v}_K \tag{3}$$

where the p_K are scalars. Left multiplying (3) by $\underset{\sim}{v}_K^T$, and using Eq. (2),

$$p_K = \underset{\sim}{y}_K^T \underset{\sim}{x} \qquad K = 1 \ldots n \quad . \tag{4}$$

Left multiplying (3) by $\underset{\approx}{A}$ and using Eqs. (1) and (4) gives:

$$\underset{\approx}{A}\,\underset{\sim}{x} = \sum_{K=1}^{n} p_K \underset{\approx}{A}\,\underset{\sim}{y}_K = \sum_{K=1}^{n} p_K \lambda_K \underset{\sim}{y}_K$$

$$= \sum_{K=1}^{n} \lambda_K \underset{\sim}{y}_K \underset{\sim}{y}_K^T \underset{\sim}{x} \quad .$$

Then, since this is true for any $\underset{\sim}{x}$,

$$\underset{\approx}{A} = \sum_{K=1}^{n} \lambda_K \underset{\sim}{y}_K \underset{\sim}{y}_K^T \tag{5}$$

which expresses the singular value decomposition of the matrix $\underset{\approx}{A}$. The inverse of $\underset{\approx}{A}$ may be defined by:

$$\underset{\approx}{A}\,\underset{\approx}{A}^{-1} = \underset{\approx}{A}^{-1}\underset{\approx}{A} = I \quad .$$

Right multiplying by any eigenvector $\underset{\sim}{y}_i$ of $\underset{\approx}{A}$ gives:

$$\underset{\approx}{A}^{-1}\underset{\approx}{A}\,\underset{\sim}{y}_i = \underset{\sim}{y}_i$$

and thus from Eq. (1),

$$\underset{\approx}{A}^{-1}\underset{\sim}{y}_i = \lambda_i^{-1}\,\underset{\sim}{y}_i \quad , \quad i = 1 \ldots n \quad . \tag{6}$$

$\underset{\approx}{A}^{-1}$ therefore has the same eigenvectors as $\underset{\approx}{A}$, with eigenvalues that are the reciprocals of those of $\underset{\approx}{A}$. The singular value decomposition of $\underset{\approx}{A}^{-1}$ may be written as:

$$\underset{\approx}{A}^{-1} = \sum_{K=1}^{n} \lambda_K^{-1}\, \underset{\sim}{y}_K \underset{\sim}{y}_K^T \quad . \tag{7}$$

A singular matrix is a matrix which has at least one zero eigenvalue, and the form of the singularity may be clearly seen from Eq. (7) -- at least one term in the sum will become infinite. This could be avoided if the summation is limited to non-zero eigenvalues, say $r < n$ of them. A pseudo-inverse of a singular matrix $\underset{\approx}{A}$, which has r non-zero eigenvalues, may be defined by:

$$\underset{\approx}{A}^{I} = \sum_{K=1}^{r} \lambda_K^{-1} \underset{\sim}{v}_K \underset{\sim}{v}_K^T \quad \text{for} \quad r \leq n \ . \tag{8}$$

In practice, tomographic reconstruction is concerned with matrices that are almost singular, i.e., some eigenvalues become very small. Using the expansion of Eq. (8) and including only eigenvalues larger than a certain minimum λ_c, an upper limit may be placed on the maximum value of any element of $\underset{\approx}{A}^{I}$. In Section 4 it will be seen that this limits the amplification of noise in the reconstruction.

3. TOMOGRAPHIC RECONSTRUCTION

Object reconstruction from axial tomograms, using the convolution theorem, has been described elsewhere[9], This Section outlines the essential points of the procedure.

The true object distribution is represented by a set of two-dimensional density distributions $o_i(x,y)$ on planes $i = 1 \ldots N_p$, parallel to the detectors, as shown in Fig. 1. Assuming that a positron emitter is to be imaged, the two detectors measure, for each event, a line on which the electron-positron annihilation took place. The tomogram t_j for plane j is constructed by intersecting all such measured lines with plane j. Thus, only intersections from the annihilations that took place in or near plane j will be in their true position. Intersections from annihilations not in the plane will be displaced by variable amounts depending on the distance of the annihilation from the plane and the direction of the event. This represents a smearing effect superimposed on the true object distribution for that plane.

Mathematically, the smearing may be expressed in terms of the point response function $h_{ij}(x,y;\ x',y')$ of the imaging system which defines the effect at a point (x,y) in plane j of a point source located at (x',y') in plane i. The total contribution of the object distribution in plane i to the point (x,y) of the tomogram for plane j is $o_i(x'y') \times h_{ij}(x,y;\ x',y')$ integrated over the whole

of plane i. Then, since a tomogram consists of contributions from all planes, the density distribution for plane j is given by:

$$t_j(x,y) = \sum_{i=1}^{N_p} \iint o_i(x',y')\, h_{ij}(x,y;x',y')dx'dy' \quad . \tag{9}$$

The integral becomes a two-dimensional convolution if the point response function h_{ij} is restricted to be space invariant, i.e., its effect on the input density $o_i(x',y')$ does not depend on the actual positions x',y' and x,y, but only on the differences x-x' and y-y'. This is achieved by limiting the data to the central region of the detectors so as to eliminate any edge or solid angle effects.

Then Eq. (9) becomes

$$t_j(x,y) = \sum_{i=1}^{N_p} \iint o_i(x',y')\, h_{ij}(x-x',y-y')dx'dy' \quad , \tag{10}$$

which is usually written:

$$t_j(\underset{\sim}{r}) = \sum_{i=1}^{N_p} \{o_i(\underset{\sim}{r}) * h_{ij}(\underset{\sim}{r})\} \quad ,$$

where * denotes convolution. After taking the Fourier transform and using the convolution theorem[10], Eq. (10) becomes

$$T_j(u_x u_y) = \sum_{i=1}^{N_p} O_i(u_x u_y)\, H_{ij}(u_x u_y) \quad . \tag{11}$$

T_j represents the Fourier transform of t_j, and u_x,u_y are the frequency space variables that correspond to the real space variables x,y. The Fourier transform of the response function is the system transfer function, and in this case is a matrix $\underset{\sim}{H}$ for each frequency component u_x,u_y.

Solving Eq. (11),

$$O_\ell(u_x u_y) = \sum_{j=1}^{N_p} T_j(u_x u_y)\, H^{-1}_{j\ell}(u_x u_y) \quad , \tag{12}$$

where $\sum_j H_{ij} H^{-1}_{j\ell} = \delta_{i\ell}$. The inverse Fourier transform of (12) then gives the two-dimensional real space distribution $o_\ell(x,y)$ for all planes $\ell = 1 \ldots N_p$.

4. AMPLIFICATION OF STATISTICAL NOISE

To understand the extent of the noise amplification problem, it is necessary to examine the system transfer function in more detail, and for that a specific form of the point response function is required. This function, which represents the appearance in plane j of an isotropic point source in that or any plane, must depend upon the shape of the acceptance aperture of the detectors. Thus, if the detector aperture is a square of side d, chosen to avoid edge and solid angle effects and the detector separation is D, the response function in plane j to a point source in plane i is a square of side $2s_{ij}\, d/D$, where s_{ij} is the distance between the planes, i.e.,

$$h_{ij}(x-x',y-y') = 1 \quad \text{if} \quad |x-x'|, |y-y'| \leq s_{ij}\, d/D$$

$$= 0 \quad \text{otherwise} \quad .$$

The system transfer function is therefore the Fourier transform of a square distribution,

$$H_{ij}(u_x,u_y) = \frac{\sin a_{ij}u_x}{a_{ij}u_x} \times \frac{\sin a_{ij}u_y}{a_{ij}u_y} \quad , \tag{13}$$

where $a_{ij} = 2\pi\, s_{ij}\, d/D$. For every frequency component (u_x,u_y), Eq. (13) is used to calculate the elements of the matrix $H_{ij}(u_x,u_y)$. After inversion and substitution into Eq. (12) with the measured tomographic distributions, the reconstructed object distribution is obtained.

Expanding the sine functions in Eq. (13) as a power series:

$$\begin{aligned} H_{ij}(u_x,u_y) &= \left(1 - \tfrac{1}{3!}\, a_{ij}^2 u_x^2 + O(a_{ij}^4 u^4)\right)\left(1 - \tfrac{1}{3!}\, a_{ij}^2 u_y^2 + O(a_{ij}^4 u^4)\right) \\ &= 1 - \tfrac{1}{6}\, a_{ij}^2 (u_x^2 + u_y^2) + O(a_{ij}^4 u^4) \qquad (14) \\ &= 1 - \tfrac{1}{6}\, (i-j)^2\, s^2 (u_x^2 + u_y^2) \left(\frac{2\pi d}{D}\right)^2 \end{aligned}$$

neglecting terms of order $(a_{ij}u)^4$ and higher. s is the distance between two adjacent planes. To this approximation, the matrix $\underset{\approx}{H}$ for a four-plane reconstruction becomes:

$$\underset{\approx}{H} = \begin{pmatrix} 1 & 1-\beta & 1-4\beta & 1-9\beta \\ 1-\beta & 1 & 1-\beta & 1-4\beta \\ 1-4\beta & 1-\beta & 1 & 1-\beta \\ 1-9\beta & 1-4\beta & 1-\beta & 1 \end{pmatrix} \tag{15}$$

where $\beta = (s^2/6)(u_x^2 + u_y^2)(2\pi d/D)^2$. It is evident from Eq.(14) that for the d.c. Fourier component $u_x = u_y = 0$, $\beta = 0$ and $\underset{\approx}{H}$ is singular with rank unity. Indeterminancy of the d.c. component is a consequence of the fact that it represents the normalization for each object plane, whereas the input tomograms are normalized to the same number of intersections. The true normalization can only be determined from an additional measurement parallel to the plane, and not from an imaging system such as in Fig. 1.

The rank of $\underset{\approx}{H}$ for small, non-zero values of β may be obtained by pivotal condensation[11]. The first step [row 2 → row 2 - (1 - β)row 1, row 3 → row 3 - (1 - 4β)row 1, etc.] reduces $\underset{\approx}{H}$ to:

$$\begin{pmatrix} 1 & 1-\beta & 1-4\beta & 1-9\beta \\ 0 & 2\beta & 4\beta & 6\beta \\ 0 & 4\beta & 8\beta & 12\beta \\ 0 & 6\beta & 12\beta & 18\beta \end{pmatrix}$$

again neglecting terms of $0(\beta^2)$. The linear dependence of the third and fourth rows on the second row is evident, and the rank of the matrix is clearly two. Thus, in addition to the exact singularity of $\underset{\approx}{H}(o,o)$, an approximate singularity of $\underset{\approx}{H}$ can be expected to persist at low frequencies, for those components for which Eq. (14) remains valid. An inverse for these matrices is in principle calculable, but the elements can become extremely large. The singularity problem decreases with increasing frequency, and in general only the low frequencies, if any, are affected. The extent of the singular region will depend upon both a_{ij} and the sampling frequency in Fourier space. The maximum sampling interval is given by the sampling theorem[12], and only a_{ij}, a factor which depends on both the plane spacing s and the stereo angle of the system, d/D, can be varied.

A small point response function for certain frequencies will not be a problem if the corresponding frequency amplitude in the tomograms is also small. However, statistical fluctuations in the amplitude will be scaled by the elements of the inverse of the transfer function, a scaling which can be reduced by limiting the magnitude of the elements. A convenient way to impose such a limit, is by making a singular value decomposition of $\underset{\approx}{H}$, as described in Section 2, and including only those eigenvalues that exceed a certain lower bound, λ_c. Since matrix near-singularity results in at least one small eigenvalue, the terms which cause the elements of the inverse to become too large will be excluded. At the same time, as much information as possible will be used by including all $\lambda_K > \lambda_c$. Thus, substituting Eq. (8) into Eq. (12):

$$O_\ell(u_x u_y) = \sum_{j=1}^{N_p} \{T_j(u_x u_y) \sum_{K=1}^{r} \lambda_K^{-1} \underset{\sim}{v}_{\ell(K)} \underset{\sim}{v}^T_{j(K)}\} \tag{16}$$

where

$$\underset{\sim}{v}_K = \begin{pmatrix} v_{1(K)} \\ \vdots \\ v_{N_p(K)} \end{pmatrix}$$

are the column eigenvectors of $\underset{\approx}{H}$ corresponding to eigenvalues λ_K. Only the $r(\leq N_p)$ eigenvalues that are greater than λ_c are included in the sum over K. Usually, for frequencies other than the first few, $r = N_p$ and all eigenvalues are included. A simple relationship between λ_c, the number of events and the number of bins, may be obtained from a study of statistical noise transfer through the imaging system.

5. STATISTICAL NOISE TRANSFER

The transfer of the statistical noise on the tomograms through the reconstruction process is complicated because the process involves a Fourier transform a summation over all planes, and an inverse Fourier transform. The transform propagates the statistical fluctuation on one bin in real space into all the frequency components. The purpose of this Section is to calculate the output statistical noise on the reconstruction in terms of the input statistical noise on the tomograms, and the system transfer function, and from this obtain the relationship between λ_c and the noise amplification factor.

The approach is similar to that used elsewhere[13] in calculating the input signal-to-noise ratio for a multiple single pinhole camera. The continuous distribution of activity within the object is approximated by a piece-wise constant, two-dimensional histogram for each plane. The measured tomogram $t_j(\underset{\sim}{r})$ for plane j is an estimate of the true distribution $\mu_j(\underset{\sim}{r})$ caused by the finite number of events and the histogramming process.

The accumulation of events in a two-dimensional histogram is a Poisson process, i.e., the probability of finding $t_j(\underset{\sim}{r})$ events in a bin $\underset{\sim}{r}$ is given by Poisson statistics[14]. The mean square error on the estimate $t_j(\underset{\sim}{r})$ is therefore

$$< n_j^2(\underset{\sim}{r}) > = E[n_i^2(\underset{\sim}{r})] = \mu_j(\underset{\sim}{r}) \simeq t_j(\underset{\sim}{r}) \quad ,$$

where < > denotes mean value and E denotes expectation value. Taking the input signal to be $t_j(\underset{\sim}{r})$ and the input noise as $[< n_j^2(\underset{\sim}{r}) >]^{\frac{1}{2}}$, the signal-to-noise ratio for the input tomograms is given by

$$\varepsilon_{in} = \sqrt{t_j(\underset{\sim}{r})} \quad .$$

Statistical noise in a histogram may be considered as an approximately stationary, random process of a type known as white noise[15]. It is uncorrelated and may be represented by a random succession of δ-functions. The power spectrum for white noise, Φ_ν, is a uniform distribution over all frequencies ν and is equal to $\tilde{\mu}$, the mean number of events per unit area. The output power spectrum from the imaging process, Eq. (12), is given by[15]:

$$\Phi_\nu(O_\ell) = \sum_{j=1}^{N_p} \Phi_\nu(T_j) |H_{j\ell}^{-1}(\nu)|^2 \quad , \tag{17}$$

where ν represents an area in Fourier space. In order to concentrate on the properties of the noise, a uniform object distribution is assumed and $\Phi_\nu(T_j)$ may be taken as $\tilde{\mu}$ for all tomograms j; Eq. (17) becomes:

$$\Phi_\nu(O_\ell) = \tilde{\mu} \sum_{j=1}^{N_p} |H_{j\ell}^{-1}(\nu)|^2 \tag{18}$$

The variance, or mean square error, on the output may be calculated from the output power spectrum, Eq. (18), using the Wiener-Khinchine theorem[10], which

states that the autocorrelation function of a process is the Fourier transform of its power spectrum. However, if the process is stationary, the autocorrelation function depends only on differences, so that the variance is given by

$$\int_{-\infty}^{\infty} \Phi_\nu d\nu \quad .$$

Substituting for Φ_ν from Eq. (18), the mean square error due to the histogramming process for the reconstructed object plane O_ℓ is

$$\tilde{\mu} \sum_{j=1}^{N_p} \int_{-\infty}^{\infty} |H_{j\ell}^{-1}(\nu)|^2 \, d\nu \quad . \tag{19}$$

The statistical fluctuation on a bin, or resolution element, for plane ℓ is found by integrating Eq. (19) over the area of the bin:

$$< n_\ell^2(\underset{\sim}{r}) > = \mu_\ell(\underset{\sim}{r}) \times C_\ell \quad . \tag{20}$$

The coefficient C_ℓ is given by

$$C_\ell = \frac{\Delta^2}{M} \sum_{j=1}^{N_p} \int_{-\infty}^{\infty} |H_{j\ell}^{-1}(\nu)|^2 \, d\nu \tag{21}$$

where M is the maximum number of events from a bin of area Δ^2. The output signal-to-noise is therefore:

$$\varepsilon_{out} = \sqrt{\frac{\mu_\ell(\underset{\sim}{r})}{C_\ell}} = \frac{\varepsilon_{in}}{\sqrt{C_\ell}} \tag{22}$$

i.e., the input ratio is scaled by $C_\ell^{-\frac{1}{2}}$. In practice, the integral in (21) is band-limited by the resolution of the detectors to a maximum frequency of Δ^{-1}. The sampling interval as given by the sampling theorem is W^{-1} for an object plane of size W in real space, so an area in Fourier space, $d\nu$, is equal to W^{-2}. Therefore, writing the integral as a sum, Eq. (21) becomes:

$$C_\ell = \frac{\Delta^2}{W^2 M} \sum_{j=1}^{N_p} \sum_{q=-Q}^{+Q} |H^{-1}_{j\ell}(q)|^2 \qquad (23)$$

where Q corresponds to the maximum frequency component. If $N_b = W/\Delta$ is the number of resolution elements in one dimension, this equation becomes, for a given frequency component, q:

$$C_\ell(q) = \frac{1}{M.N_b^2} \sum_{j=1}^{N_p} |H^{-1}_{j\ell}(q)|^2 \quad ,$$

and substituting the singular value decomposition for $\underset{\approx}{H}^{-1}$ gives

$$C_\ell(q) = \frac{1}{M.N_b^2} \sum_{j=1}^{N_p} \left| \sum_{K=1}^{r} \lambda_K^{-1} \, v_{\ell(K)}(q) \, v^T_{j(K)}(q) \right|^2 \quad . \qquad (24)$$

Normalization of the eigenvectors ensures that all terms in the numerator of Eq. (24) are $\lesssim 1$. As explained previously, the factor λ_K in the denominator can become $<< 1$, unless a lower limit is imposed. It is clear from Eq. (24) that a limit such that $M.N_b^2\lambda_K^2 \sim 1$ is appropriate, although an exact value for each term will also depend upon the eigenvectors. The over-all effect must be to keep C_ℓ as small as possible to avoid reducing the signal-to-noise ratio according to Eq. (22).

To summarize, a significant reduction in the output signal-to-noise ratio may be avoided if the singular value decomposition is limited to include only those eigenvalues larger than a minimum λ_c, given by:

$$\lambda_c \sim \frac{1}{N_b\sqrt{M}} \quad . \qquad (25)$$

This minimum value involves both a factor dependent on the detector resolution ($N_b \equiv$ bin width for fixed object dimensions) and a statistical factor ($\sqrt{M}$) that depends on the amount of data taken.

6. APPLICATION TO A SIMULATED POSITRON CAMERA

The reconstruction method was tested on simulated data from a positron camera. The camera consisted of two position-sensitive detectors 20 cm apart with a square acceptance aperture of 7 cm. The objects were reconstructed on planes spaced 2 cm apart, and each plane consisted of 32 × 32 bins, 2 mm square.

The output from the imaging process consisted of a set of tomograms for each input distribution, and the reconstruction attempted to recover this original distribution from the tomograms. The input distributions contained ∿ 100 events/bin, and the value for λ_c from the results of the previous Section would be

$$\lambda_c \sim \frac{1}{32 \times 10} \simeq 3 \times 10^{-3} \quad .$$

The precise value is not important because the eigenvalues are discrete and widely spaced. Thus $\lambda_c \sim 3 \times 10^{-3}$ excludes, for example, in the case of $\underset{\sim}{H}(1,0)$ only one out of five eigenvalues.

The source to be imaged consisted of events distributed uniformly according to the shape of the letters A, B and C on three adjacent planes. The reconstructions are shown in Fig. 2, for the three planes containing the letters, and an empty plane. The first row shows the unmodified tomograms; the clarity of the letters is a result of the artificially high object contrast, but for imaging purposes the effective elimination of the background is a more important consideration. The second row illustrates the "brute force" method where the frequency amplitude is unmodified if the corresponding determinant of $\underset{\sim}{H}$ is less than a fixed value. Since the determinant of $\underset{\sim}{H}$ can be written[11]:

$$\det \underset{\sim}{H} = \prod_{K=1}^{N_p} \lambda_K \quad ,$$

this procedure is equivalent to singular value decomposition with r = 0 if $\det \underset{\sim}{H}$ is less than a cut-off. The remaining two rows of Fig. 2 correspond to values of λ_c of 0.5 and 10^{-2}, respectively.

The results clearly show the importance of correct modification of the low frequencies, if the background is to be cleanly removed. No modification leaves a substantial smearing in the final image (second row). Too large a cut-off removes some of this background, but a low frequency hump or depression (depending on the

plane) still remains (third row). Too small a cut-off causes over-correcting of low frequencies leading to a dip in the centre and an accumulation of events in the corners. However, a properly adjusted value of λ_c results in an almost flat background, particularly in the empty planes (fourth row). The number of events in the empty planes can never be zero because, as was mentioned in Section 4, the true normalization for each plane cannot be determined by this method.

The reconstruction has also been successfully used to treat real data taken for an extended positron source with a recently-developed proportional chamber positron camera[16]. The results will be the subject of a further paper.

ACKNOWLEDGEMENT

We would like to thank E. Edberg, N. Ford and B. Schorr for helpful discussions.

REFERENCES

1) See:
R.A. Brooks and G. di Chiro, Review Article on Principles of Computer Assisted Tomography (CAT) in Radiographic and Radioisotropic Imaging, Phys. Med. Biol. (1976), Vol. 21, No. 5.

2) H.O. Anger, Fundamental Problems in Scanning (Ed. A. Gottschalk and R.N. Beck, Springfield: C. Thomas) (1968), pp. 195-211.

3) See, e.g.,
IEEE Transactions on Nuclear Science NS-21, No. 3 (1974).

4) H.H. Barrett, Fresnel Zone Plate Imaging in Nuclear Medicine, J. Nucl. Med. v. 13, No. 6 (1972).

5) H.O. Anger, Gamma-Ray and Positron Scintillation Camera, Nucleonics v. 21, No. 10 (1963).

6) J.M.S. Prewitt, "Object Enhancement and Extraction", in Picture Processing and Psychopictorics, Academic Press (1970).

7) D.R. Dance, B.C. Wilson and R.P. Parker, Phys. Med. Biol. Vol. 20, No. 5 (1975).

8) C.R. Rao and S.K. Mitra, Generalized Inverse of Matrices and its Applications (J. Wiley and Sons) (1971).
E. Edberg, Matrix Computation, CERN Yellow Report 76-22 (1976).

9) L.T. Chang, B. Macdonald and V. Perez-Mendez, Lawrence Berkeley Laboratory Report 3872 (1975).

10) D.C. Champency, Fourier Transforms and their Physical Applications, Ch. 5 (Academic Press) (1973).

11) A.C. Aitken, Determinants and Matrices (Oliver and Boyd) (1972).

12) Notes on Analogue-Digital Conversion Techniques (Ed. A.K. Susskind), Ch. II (Technology Press of Massachusetts Institute of Technology and John Wiley & Sons) (1957).

13) L.T. Chang, Ph.D. Thesis, Lawrence Berkeley Laboratory Report 4887 (1976), Appendix B.

14) W.T. Eadie, D. Drijard, F.E. James, M. Roos and B. Sadoulet, Statistical Methods in Experimental Physics (North Holland) (1971).

15) C.W. Helstrom, Statistical Theory of Signal Detection (Pergamon Press) (1968).

16) A.P. Jeavons and C. Cate, IEEE Trans. Nucl. Sci. NS-23, p. 640 (1976).

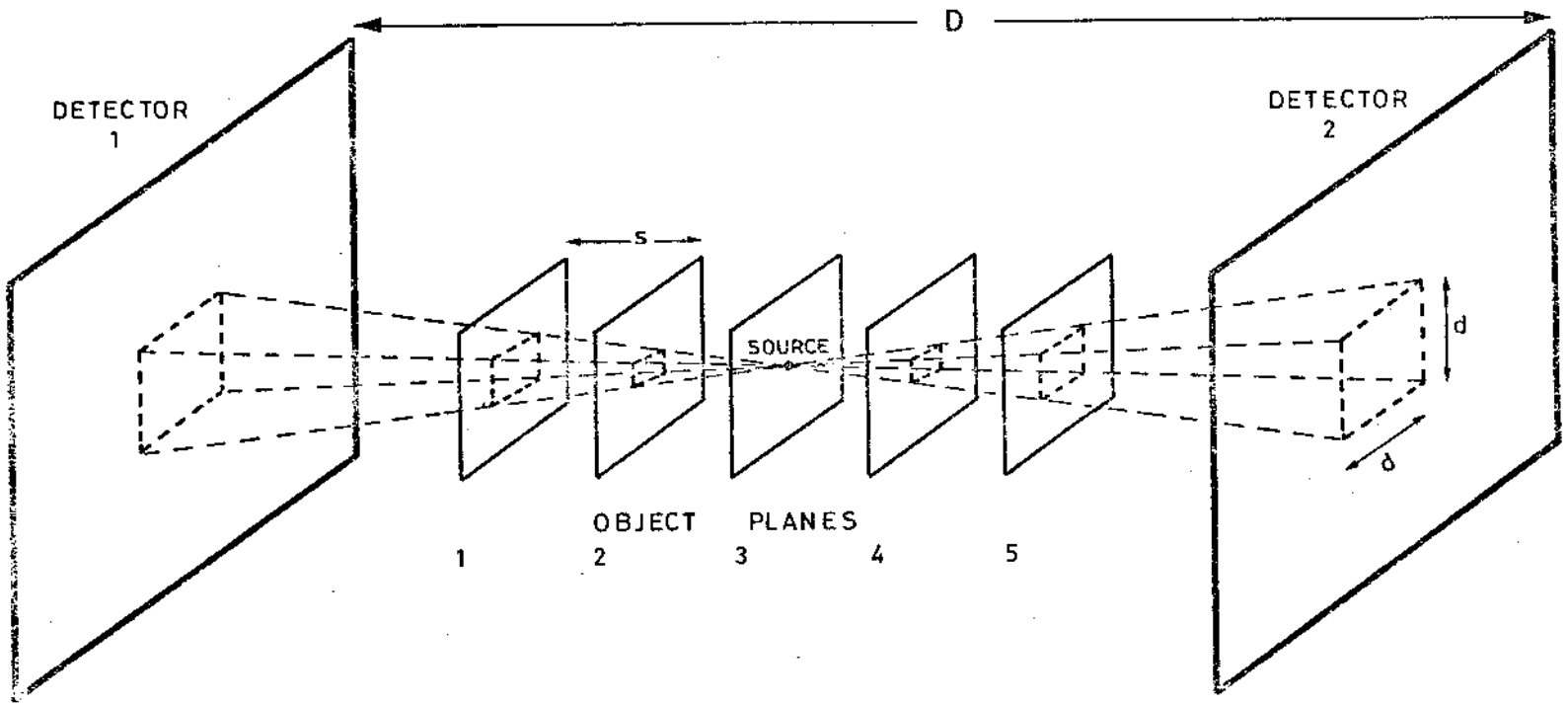

Fig. 1 – Schematic layout of Positron camera

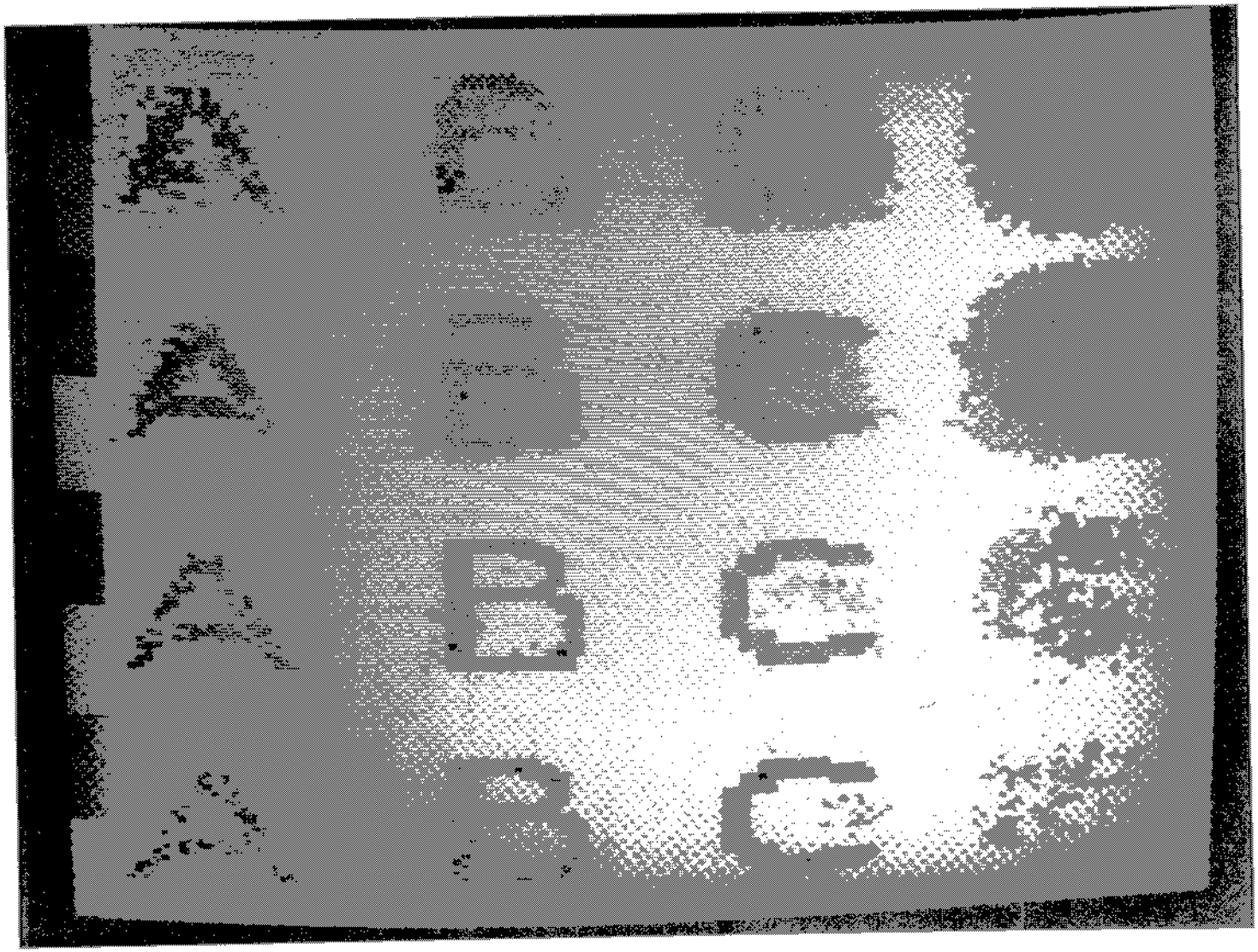

(a) original tomograms;

(b) no low frequency correction;

(c) $\lambda_c = 0.5$;

(d) $\lambda_c = 10^{-2}$.

Fig. 2 - Reconstruction of extended object for planes 2, 3, 4 and 5; the object planes are 2(A), 3(B) and 4(C).